human reproduction

ORIGINAL ARTICLE *Reproductive genetics*

Differentiation of primordial germ cells from induced pluripotent stem cells of primary ovarian insufficiency

Lizhi Leng[1,2], Yueqiu Tan[1,2], Fei Gong[1,2], Liang Hu[1,2,3], Qi Ouyang[1,2,3], Yan Zhao[3], Guangxiu Lu[1,2,3,*], and Ge Lin[1,2,3,*]

[1]Institute of Reproductive & Stem Cell Engineering, Central South University, Changsha 410078, China [2]Key Laboratory of Stem Cells and Reproductive Engineering, Ministry of Health, Changsha 410078, China [3]National Engineering and Research Center of Human Stem Cell, Changsha 410078, China

*Correspondence address. Tel: +86-731-84805319 (G.L.)/+86-731-82355100 (G.X.L.); Fax: +86-731-84497661 (G.L.)/+86-731-84497661 (G.X.L.); E-mail: linggf@hotmail.com (G.L.)/lugxdirector@aliyun.com (G.X.L.)

STUDY QUESTION: Can the induced pluripotent stem cells (iPSCs) derived from women with primary ovarian insufficiency (POI) differentiate into germ cells for potential disease modeling *in vitro*?

SUMMARY ANSWER: The iPSC lines derived from POI patients with 46, X, del(X)(q26) or 46, X, del(X)(q26)9qh+ could differentiate into germ cells and expressed lower levels of genes in the deletion region of the X chromosome.

WHAT IS KNOWN ALREADY: iPSC technology has been envisioned as an approach for generating patient-specific stem cells for disease modeling and for developing novel therapies. It has also been confirmed that iPSCs differentiate into germ cells.

STUDY DESIGN, SIZE, DURATION: We compared the differentiation ability of germ cells and the gene expression level of germ cell-related genes in the X chromosome deletion region of iPSC lines derived from POI patients ($n = 2$) with an iPSC line derived from normal fibroblasts ($n = 1$).

PARTICIPANTS/MATERIALS, SETTING, METHODS: We established three iPSC lines from two patients with partial Xq deletion-induced POI and normal fibroblasts by overexpressing four factors: octamer-binding transcription factor 4 (*OCT4*), sex-determining region Y-box 2 (*SOX2*), Nanog homeobox (*NANOG*), and lin-28 homolog (*LIN28*), using lentiviral vectors. We then generated stable-transfected fluorescent reporter cell lines under the control of the Asp-Glu-Ala-Asp box polypeptide 4 (*DDX4*, also called *VASA*) promoter, and selected clonal derived sublines. We induced subline differentiation into germ cells by adding Wnt3a (30 ng/ml) and bone morphogenetic protein 4 (100 ng/ml). After 12 days of differentiation, green fluorescent protein (GFP)-positive and GFP-negative cells were isolated via fluorescence-activated cell sorting and analyzed for endogenous VASA protein (immunostaining) and for germ cell markers and genes expressed in the deleted region of the X chromosome (quantitative RT–PCR).

MAIN RESULTS AND THE ROLE OF CHANCE: The POI- and normal fibroblast-derived iPSCs had typical self-renewal and pluripotency characteristics. After stable transfection with the VASA-GFP construct, the sublines POI1-iPS-V.1, POI2-iPS-V.1 and hEF-iPS-V.1 produced green fluorescent cells in the differentiated cultures, and the percentage of GFP-positive cells increased over the 12 days of differentiation to a maximum of $6.9 \pm 0.33\%$, $5.3 \pm 0.57\%$ and $8.5 \pm 0.29\%$, respectively, of the total cell population. Immunohistochemical analysis confirmed that endogenous VASA was enriched in the GFP-positive cells. Quantitative reverse transcription-PCR revealed significantly higher expression of germ cell markers [PR domain containing 1, with ZNF domain (*PRDM1*, *BLIMP1*), developmental pluripotency-associated 3 (*DPPA3*, *STELLA*), deleted in azoospermia-like (*DAZL*), and *VASA* (*DDX4*)] in GFP-positive cells than in GFP-negative cells. Moreover, the GFP-positive cells from POI-iPSCs had reduced expression of the family with sequence similarity 122C (*FAM122C*), inhibitor of kappa light polypeptide gene enhancer in B-cells, kinase gamma (*IKBKG*), and RNA binding motif protein, X-linked (*RBMX*), genes located in the deleted region of the X chromosome and that are highly expressed in differentiated germ cells, compared with cells from normal iPSCs.

LIMITATIONS, REASONS FOR CAUTION: Gene expression profiling indicated that the germ cells differentiated from POI-iPSCs were pre-meiotic. Therefore, how the differentiated primordial germ cells could progress further to meiosis and form follicles remains to be determined in the study of POI.

Introduction

Primary ovarian insufficiency (POI), also termed premature ovarian failure (POF), is characterized by primary or secondary amenorrhea of >4–6-month duration before the age of 40 years. LH and FSH are elevated (FSH > 40 mIU/ml), and estrogen is in the menopausal range (Coulam, 1982). The incidence of POI is increasing and is prevalent in up to 1–3% of females (Christin-Maitre and Braham, 2008). Currently, POI is one of the main diseases causing female infertility and threatening women's health. However, there are few effective methods for treating POI. Estrogen and progestin hormone replacement therapy or oocyte donation are used in the clinic to alleviate the post-menopausal symptoms and for egg donation cycles in patients with POI. Nevertheless, both approaches have their own limitations: the former can only improve rather than cure the ovaries; the latter faces the prospect of donated oocyte shortage. Therefore, further understanding of the disease is required to develop new strategies for treating POI effectively.

Chromosomal abnormalities have been acknowledged as a frequent cause of POI (Castillo *et al.*, 1992; Portnoi *et al.*, 2006; Ceylaner *et al.*, 2010; Janse *et al.*, 2010; Baronchelli *et al.*, 2011; Jiao *et al.*, 2012; Rao Kandukuri et al., 2012). Overall, X chromosome abnormalities, especially Xq terminal deletions, are the most frequently detected in the clinic (Jiao *et al.*, 2012). It has been shown that X chromosome deletion could result in primary or secondary amenorrhea (Forges *et al.*, 2006; Nippita and Baber, 2007; Sinha and Kuruba, 2007). These observations suggest that critical genes for normal ovarian development and function are located on the X chromosome (Cordts et al., 2011). Moreover, cytogenetic and molecular analyses of women with POI with balanced X-autosome translocation have defined two critical regions for POF: POF1 Xq26-Xqter (Tharapel *et al.*, 1993) and POF2 Xq13.3-Xq21.1 (Sala *et al.*, 1997). Haploinsufficiency or disruption of genes in these regions may explain why X chromosome deletions and translocations affect ovarian function (Davison et al., 2000). In addition, heterochromatin rearrangements of the Xq13-Xq21 region down-regulate oocyte-expressed genes during oocyte and follicle maturation, indicating that X-linked POI may also derive from epigenetic alterations (Rizzolio et al., 2009).

X chromosome deletions, translocations, or mutations in POI patients have been used to identify genes or gene regions involved in ovarian development and/or ovarian maintenance. X-linked genes associated with POI include dachshund family transcription factor 2 (*DACH2*), membrane-bound X-prolyl aminopeptidase (aminopeptidase P) 2 (*XPNPEP2*) (Prueitt *et al.*, 2002), progesterone receptor membrane component 1 (*PGRMC1*) (Mansouri *et al.*, 2008), choroideremia (Rab escort protein 1) (*CHM*) (Lorda-Sanchez *et al.*, 2000), collagen type IV, alpha 6 (*COL4A6*)

(Nishimura-Tadaki *et al.*, 2011), premature ovarian failure 1B (*POF1B*) (Bione *et al.*, 2004), diaphanous-related formin 2 (*DIAPH2*) (Bione *et al.*, 1998), and fragile X mental retardation 1 (*FMR1*) (Gleicher *et al.*, 2009). However, with the exception of *PGRMC1* and *FMR1*, most of these genes have not been investigated for molecular perturbations. Mutation screening and RNA expression studies of *PGRMC1* have shown that mutant or reduced *PGRMC1* may cause POI through impaired activation of the microsomal cytochrome P450 and increased apoptosis of ovarian cells (Mansouri *et al.*, 2008). *FMR1* is expressed in oocytes and encodes an RNA-binding protein involved in translation (Rife *et al.*, 2004). Another study suggested that *FMR1* served a special function during germ cell proliferation (Bachner *et al.*, 1993).

Despite extensive studies on POI-related X chromosome abnormalities, the X chromosome abnormality link to POI phenotypes and molecular mechanisms remains unclear due to the lack of adequate and convenient experimental models. Current studies envisioned cellular reprogramming and the generation of induced pluripotent stem cells (iPSCs) from adult cell types as approaches to generating patient-specific stem cells for studying disease mechanisms and developing specific therapies. To date, iPSCs derived from the somatic cells of various disorders have been used in disease models. Some examples include amyotrophic lateral sclerosis (Dimos *et al.*, 2008), Rett syndrome (Marchetto et al., 2010), spinal muscular atrophy (Ebert *et al.*, 2009), Angelman syndrome (Chamberlain *et al.*, 2010) and Timothy syndrome (Pasca *et al.*, 2011). When differentiated into disease-relevant cell types, most of the iPSCs manifested observable disease-specific phenotypes. In this study, we generated iPSC lines from two POI patients with terminal Xq deletions and explored their potential for germ cell differentiation.

Materials and Methods

Patients

We included two women with POI in this study. They donated skin samples for iPSC derivation and late differentiation study after providing written informed consent. The CITIC-Xiangya Reproductive and Genetic Hospital ethical committee approved the study. The history of these patients is detailed below.

Case 1

A 28-year-old woman was referred with a history of secondary amenorrhea. Her onset of menarche was at the age of 14 years and she had regular menstrual periods from age 15–22 years; the menstrual period duration was 27–28 days. She had unexplained amenorrhea at the age of 23 years. Endocrinological examination revealed elevated serum FSH of 64.59 mIU/ml (normal range: 3–20 mIU/ml) and LH of 39.25 mIU/ml (normal range: 0.8–10.4 mIU/ml), and normal estradiol (E2) of 48.70 pg/ml (normal

range: 10–77 pg/ml). Her external genitalia were normal. Pelvic ultrasound revealed small bilateral ovaries without obvious follicles. Chromosomal Giemsa (G)-band analyses revealed a 46, X, del(X)(q26) karyotype.

Case 2

A 34-year-old woman was referred with a history of secondary amenorrhea. Her onset of menarche at the age of 14 years and she complained of irregular menstrual cycles of 1–2 times per year since the age of 15 years. Amenorrhea began at the age of 17 years. Endocrinological examination revealed elevated serum FSH of 64.02 mIU/ml and LH of 34.56 mIU/ml, and decreased E2 of 5.0 pg/ml. Her external genitalia were normal. Pelvic ultrasound revealed small bilateral ovaries without obvious follicles and a small uterus. Chromosomal G-band analyses revealed a 46, X, del(X)(q26)9qh+ karyotype.

Derivation of primary fibroblast cells

Human dermal fibroblasts were derived from the skin via operative incision under local anesthetic. The skin tissues were digested into cell aggregates and plated onto Matrigel-coated tissue culture dishes for adherent culture with Dulbecco's modified eagle medium (DMEM; HyClone, USA) containing 10% (v/v) fetal bovine serum (FBS; Gibco, New York, USA). Typical fibroblast cells grew and migrated out of the aggregates after 2–3 days. Normal human embryonic fibroblasts (hEFs) were obtained from the National Engineering and Research Center of Human Stem Cell (Zhou et al., 2008).

Lentiviral transduction and iPS cell generation

The day before transduction, 293FT cells were seeded at 3×10^6 cells per 6-well plate. On the next day, four lentiviral vectors [pSin-EF2-Oct4-Pur (Plasmid 16579), pSin-EF2-Sox2-Pur (Plasmid 16577), pSin-EF2-Nanog-Pur (Plasmid 16578), pSin-EF2-Lin28-Pur (Plasmid 16580), all purchased from Addgene (Addgene, Massachusetts, USA), were introduced into 293FT cells in similar concentrations by Lipofectamine 2000 (Invitrogen, Carlsbad, CA, USA) according to the manufacturer's instructions. The inserted size of the four lentiviral vectors was 600, 900, 1000 and 1100, respectively. After 36 h, virus-containing supernatants generated from 293FT cultures were filtered through a 0.45-μm filter (Millipore, Boston, MA, USA) and supplemented with 8 μg/ml polybrene (Sigma-Aldrich, USA). For iPSC derivation, human fibroblast cells were incubated in the virus/polybrene-containing supernatants overnight. After infection, the cells were digested into single cell suspensions and replated onto irradiated mouse embryonic fibroblasts (MEFs). The culture medium was replaced with DFSR medium [DMEM/F12 supplemented with 15% (v/v) knockout serum replacer (knockout SR, Batch numbers: 942630, 1001565, 1036840 and 1099211), 2 mM L-glutamine, 2 mM non-essential amino acids, 0.1 mM β-mercaptoethanol, 4 ng/ml human basic fibroblast growth factor (bFGF) (all from Invitrogen)]. The medium was changed every other day. Fifteen or twenty days after infection, clones were picked up and plated onto MEFs in 6-well plates for culture using standard procedures (Lin et al., 2009).

iPSC culture and stable transfection with reporter construct

The VASA-GFP reporter was gifted by Professor Renee A. Reijo Pera (Stanford University, USA) and was prepared as above. POI-iPSC and hEF-iPSC clones were released from the feeder layers by mechanical cutting and transferred onto Matrigel-coated 6-well plates. The cells were cultured with conditioned medium (CM, DFSR medium collected after overnight incubation on irradiated MEFs) supplemented with 10 ng/ml bFGF. After 24 h, the medium was replaced with supernatant containing VASA-GFP reporter and 8 μg/ml polybrene. The selection of stable transformants was based on the expression of the bacterial neomycin phosphotransferase gene (neo) under the control of the simian virus 40 (SV40) promoter. POI-iPSC and hEF-iPSC

clones resistant to geneticin (200 μg/ml) were selected after 15 days. Undifferentiated iPSC cultures were maintained with CM plus 10 ng/ml bFGF during selection. After selection, the remaining cells were digested into single cell, which were picked up and transferred onto MEFs in 24-well plates (one cell per well) to prepare sublines. The sublines were tested for the presence of the VASA-GFP construct by PCR using genomic DNA (gDNA) as the template and two sets of primers spanning the insert promoter sequence into the GFP and nested in the GFP coding sequence. Additionally, we checked the function of the reporter system by inducing differentiation of positive sublines and monitoring the reporter gene fluorescence under fluorescence microscopy during the time course. POI1-iPS-V.1, POI2-iPS-V.1 and hEF-iPS-V.1 VASA-GFP-transduced sublines were used throughout this analysis.

Primordial germ cell differentiation

POI1-iPS-V.1, POI2-iPS-V.1 and hEF-iPS-V.1 cells were detached from the feeder layers and suspended for 24 h in DFSR medium without bFGF to form embryoid bodies (EB). For primordial germ cells (PGCs) differentiation, EBs were initially cultured in DFSR medium containing 30 ng/ml Wnt3a (2324-WN; R&D, Minneapolis, MN, USA) for 24 h, and then the medium was changed to DFSR medium supplemented with 100 ng/ml bone morphogenetic protein 4 (BMP4, 314-BP; R&D, Minneapolis, MN, USA) for another 24 h. Subsequently, the EBs were plated on Matrigel-coated 6-well plates and cultured in DFSR medium containing 100 ng/ml BMP4. The medium was replaced every other day in the subsequent 14-day differentiation (Fig. 3A). The emergence of green fluorescent cells was monitored every 2 days by epifluorescence microscopy. Samples were collected on Day 8, 10, 12, 14 and 16 for fluorescence-activated cell sorting (FACS).

In vivo and in vitro differentiation

For the in vivo differentiation assay, $0.5 – 1 \times 10^6$ iPSCs were collected and injected intramuscularly into the leg of 6–8-week-old non-obese/severe combined immunodeficiency (NOD-SCID) mice. About 2 months later, the xenografts were collected for histological analysis by hematoxylin and eosin (H&E) staining. Anti-human nuclei antibody was used for immunofluorescence staining to identify human cell origin of the teratomas.

For the in vitro differentiation assay, iPSCs were harvested by treating with 1 mg/ml collagenase IV(Gibco, New York, USA). The clumps of the iPSCs were transferred to bacterial culture dishes in the DFSR medium without bFGF to form embroid bodies (EBs). After 10 days as a floating culture, EBs were collected and replated onto matrigel-coated 6-well plates for an additional 5 days for immunofluorescence analysis. Meanwhile, the attached cells were then collected for quantitative RT–PCR to detect the expression of lineage markers representing the three germ layers.

Alkaline phosphatase activity and immunofluorescence staining

We detected alkaline phosphatase (AKP) activity using a Fast Red Substrate Pack (Zymed Laboratories, South San Francisco, USA) according to the manufacturer's protocol. For immunofluorescence staining, cells were fixed for 15 min in 4% (w/v) paraformaldehyde in phosphate-buffered saline (PBS) at room temperature, and then blocked with PBS containing 0.25% (v/v) Triton X-100 (Sigma-Aldrich), 4% (v/v) goat serum or 10% (v/v) donkey serum, and 1% (v/v) bovine serum albumin at room temperature for 30 min. After blocking, the cells were incubated with primary antibodies (diluted in blocking buffer) overnight in a humidified chamber at 4°C, followed by incubation with secondary antibodies at room temperature in the dark for 1 h. Between each step, the cells were washed with PBS. We used the following antibodies: mouse anti-octamer-binding transcription factor (OCT) 3/4 (OCT3/4, 1:50, sc5279; Santa Cruz, California, USA), mouse anti-stage-

specific embryonic antigen 4 (SSEA4, 1:50, MAB1435; R&D, Minneapolis, MN, USA), mouse anti-TRA-1-60 (1:50, MAB4360; Chemicon, California, USA), mouse anti-β-tubulin (1:800, T8660; Sigma-Aldrich, Pittsburgh, USA), mouse anti-smooth muscle antigen (SMA, 1:100, CBL171; Chemicon, California, USA), goat anti-sex-determining region Y-box 17 (SOX17, 1:100, AF1924; R&D, Minneapolis, MN, USA), mouse anti-human nuclei (1:200, MAB1281; Millipore), and goat anti-VASA (2 μg/ml, AF2030; R&D, Minneapolis, MN, USA). We visualized antigen localization using goat anti-mouse Alexa Fluor 488 (1:1000, A11017), donkey anti-goat Alexa Fluor 488 (1:1000, A11055) and goat anti-rabbit Alexa Fluor 488 (1:1000, A11070; all from Invitrogen). Nucleuses were stained with diamidino-phenylindole (DAPI, 1 μg/ml, D1306; Invitrogen).

Semiquantitative and quantitative reverse transcription–PCR

Total RNA was extracted with TRIzol (Invitrogen). We synthesized complementary DNA (cDNA) using 1 μg total RNA in a 20-μl reaction using a RevertAid First Strand cDNA Synthesis Kit (Fermentas Life Sciences, Burlington, Canada) according to the manufacturer's instructions. Semiquantitative reverse transcription (RT)-PCR was carried out under the following conditions: 5 min at 95°C; 30 cycles of 30 s at 94°C, 30 s at 56–61°C, 30 s at 72°C, and 5-min extension at 72°C. Quantitative PCR reactions were performed with FastStart Universal SYBR Green Master (Roche, Basal, Switzerland). The transcript levels were determined by using the Roche LightCycler 480 II System (Roche, Basal, Switzerland). We used glyceraldehyde-3-phosphate dehydrogenase (*GAPDH*) as the internal standard, and calculated the average comparative threshold cycle (ΔCt) values for analysis. Supplementary Table SI lists the primers used.

Transgene copy number analysis

To examine the integrated copies of transgenes (*OCT4*, *SOX2*, *NANOG* and *LIN28*) in iPS clones, genomic DNA was purified and primers specific for each transgene were used to analyze the established iPS clones. Real-time quantitative PCR reactions were performed using 25 ng of gDNA with the

FastStart Universal SYBR Green Master and run on a Roche LightCycler 480 II System. The relative copy numbers of the four transgenes in iPSCs were calculated according to the relative quantity of endogenous genes to β-globin in origin fibroblasts. The primers are provided in Supplementary Table SI.

Flow cytometry analysis

Adherent cells were harvested by trypsin treatment (0.05% (w/v) Trypsin/0.5 mM EDTA, Invitrogen, USA). The treated cells were fixed in 4% (w/v) paraformaldehyde for 10 min at room temperature (RT) and then filtered through a 40-μm mesh. About 1×10^6 cells were used in Stage-specific embryonic antigen (SSEA-4, 1:40, MAB1435; R&D, Minneapolis, MN, USA) labeling. Both primary and secondary antibody incubation were carried out at room temperature for 1 h. Control samples were stained with IgG_3 (1:100, MAB007; R&D, Minneapolis, MN, USA). After washing, the cells were re-suspended in 500 μl of FACS buffer [PBS containing 1% (v/v) FBS and 0.1% (w/v) sodium azide], and proceeded for analysis on a Becton Dickinson FACSAria (FACSARIA, BD Biosciences, San Diego, CA, USA). A total of 10 000 events were acquired. For Fluorescence-Activated Cell Sorting of VASA-GFP positive cells, differentiated cells were incubated with 1 mg/ml of Collagenese IV for 10 min and with trypsin for 20 min by periodic pipetting to yield single cell suspensions. Cells were collected by centrifugation (600 g for 5 min), washed twice with FACS buffer, and then re-suspended in FACS buffer (1 ml). GFP positive and negative cells were sorted using a Becton Dickinson FACS with exclusion of cell debris. Sorted cells were pelleted by centrifugation (600 g for 5 min) and then used for subsequent analysis. The overall experimental design is illustrated in Fig. 1.

Telomerase activity assay

Quantitative measurement of telomerase activity (TRAP assay) was performed using the TRAPeze Telomerase detection kit or TRAPeze RT Telomerase detection kit (Millipore). Briefly, the cells were lysed on ice for 30 min in CHAPS buffer and then centrifuged at 12 000 g for 20 min at 4°C. The supernatant was collected and the protein concentrations were
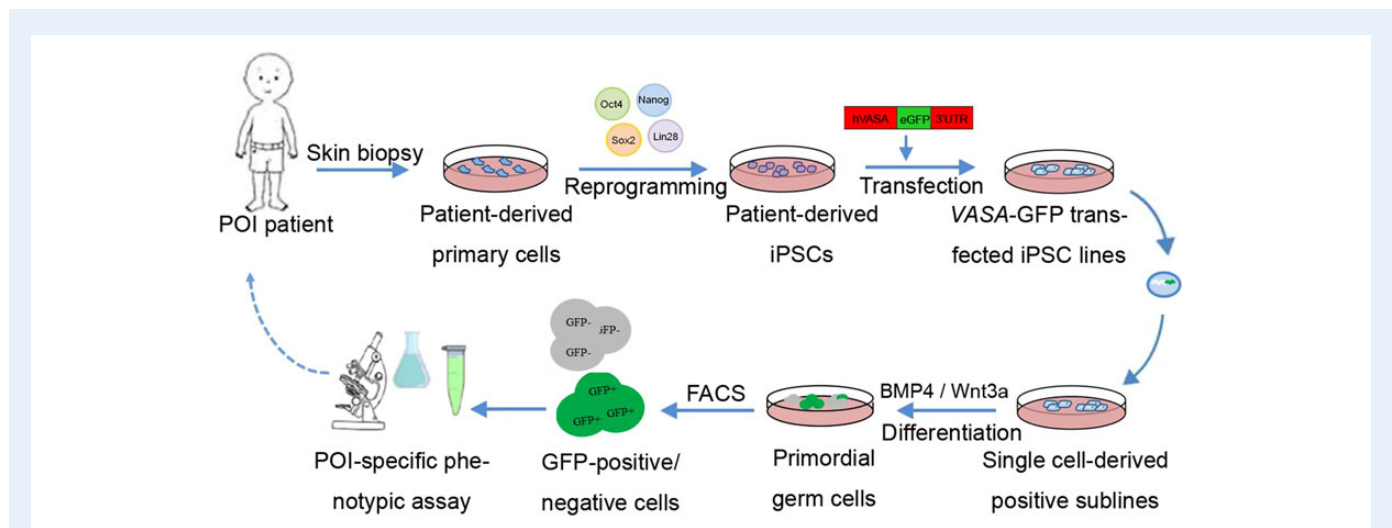

Figure 1 Primary ovarian insufficiency (POI) disease modeling using induced pluripotent stem cell (iPSC) technology. iPSC-based disease model generation begins with cells isolated from POI patients by skin punch biopsy. Upon reprogramming, POI-iPSC clones are selected, expanded and characterized. Undifferentiated POI-iPSCs are stably transfected with an Asp-Glu-Ala-Asp box polypeptide 4-green fluorescent protein (VASA-GFP) construct. After that, clonal derived sublines are selected. Sublines are induced to differentiate into germ cells *in vitro*. After 12 days of differentiation, GFP-positive and GFP-negative cells were isolated with a fluorescence-activated cell sorter (FACS) and analyzed for the expression of VASA protein, early germ cell markers, and genes located in Xq26.3-q28.

determined by bicinchoninic acid (BCA) protein assay. The TRAP assay was carried out according to the manufacturer's instructions, using a total of 200 ng protein in each reaction. Telomerase activity was determined by electrophoresis of the PCR products in a 12.5% (w/v) non-denaturing polyacrylamide gel with silver staining, or by fluorometric detection and real-time quantification of the PCR products using an ABI Prism 7500.

Karyotype analysis

The iPSC clones were transferred onto Matrigel-coated dishes for propagation and prevention of MEF contamination. After 2−3 passages, cells were treated with demecolcine solution (Sigma-Aldrich, Pittsburgh, USA) for 2.5 h and then used in standard G-banding karyotype analysis. The analysis was based on 50 metaphase cells per sample.

Array comparative genomic hybridization

We performed array comparative genomic hybridization (aCGH) assays (Cytochip Focus constitutional, BlueGnome, Cambridge, UK) based on the principle of competitive hybridization. Based on the manufacturer's protocol, gDNA was digested into 200−500-bp fragments, random prime−labeled with cyanine-5/cyanine 3-dUTP, mixed, and precipitated. Then, gDNA was hybridized on array slides for 17−21 h, and the slides were washed with 2 × standard saline citrate/0.05% (v/v) Tween 20. Lastly, the slides were scanned using a 10-μm laser scanner (Innopsys 710A; Innopsys, France) and the images analyzed (BlueFuse Multi software; BlueGnome, Cambridge, UK). We analyzed the aCGH ratio plots of each gDNA sample for gains and losses, and predicted the normal/abnormal status of the corresponding cells.

Statistical analysis

Independent sample t-tests between groups were used to evaluate the statistical significance of mean values by using SPSS 18.0 for Windows. Homogeneity of variance was analyzed before the independent sample t-test, in which statistical significance levels of the two variance estimates was $P > 0.1$. If the variance was not equal, unequal-variances t-test was used. Statistical significance levels were $P < 0.05$ (denoted as *). All P values were two-tailed.

Results

Derivation and characterization of iPSC lines

We established fibroblast cell lines from the skin tissues of two POI patients, designating them POI1 and POI2; normal human fibroblasts were termed hEF. To generate iPSCs, we introduced lentiviruses containing human OCT4, Nanog homeobox (NANOG), SOX2 and lin-28 homolog (LIN28) into the three fibroblast cell lines. Approximately 7 days after transduction, small cell colonies clearly distinguishable from the fibroblast cells began to appear. Clones with human embryonic stem cell (hESC) morphology first became visible at Day 15. At around 20 days, the clones had become tightly packed and each cell in the colony had a high nuclear-to-cytoplasmic-ratio morphology similar to that of hESCs (Supplementary Fig. S1). The reprogramming efficiency of POI1, POI2 and hEF was 0.0064 ± 0.0027%, 0.0081 ± 0.0092% and 0.0077 ± 0.0054%, respectively.

The generated iPSC colonies shared similar characteristics to hESC. All the iPS cells were positive for AP activity and expressed the pluripotent-specific surface antigens SSEA-4 and TRA-1-60, and the nuclear transcription factor OCT4 (Fig. 2A). Moreover, semiquantitative RT−PCR showed that all iPSCs expressed the pluripotency-associated genes, including OCT4, NANOG, SOX2, RNA exonuclease 1 homolog

(REX1), left-right determination factor (LEFTY), Thy-1 cell surface antigen (THY1), and telomeric repeat binding factor (NIMA-interacting) 1 (TERF1) when compared with a previously established hESCs (Fig. 2C).

Three clones (POI1-iPSCs, POI2-iPSCs, and hEF-iPSCs) with minimal differentiation were successfully selected for continuous expansion up to 50 passages, which maintained undifferentiated states during in vitro culture as detected by surface marker SSEA-4 at 40 to 50 passages (Supplementary Fig. S2A). POI1-iPSCs, POI2-iPSCs and hEF-iPSCs also expressed high telomerase activity (Supplementary Fig. S2B), which reflect their immortal replication ability. We did not observe discernible differences in the self-renewal and pluripotent markers of the reprogrammed cells derived from POI patients and healthy donors.

Next, we evaluated the developmental potential of the established iPSCs through both in vitro and in vivo assays. Various types of cells grew out of EBs after attachment. Immunofluorescence staining revealed the presence of cells expressing ectoderm (β-tubulin), mesoderm (SMA) and endoderm (SOX17) markers (Fig. 2B). Also, quantitative RT−PCR results showed that paired box 6 (PAX6) and NESTIN (ectoderm), kinase insert domain receptor (KDR, FLK1) and heart and neural crest derivatives expressed 1 (HAND1) (mesoderm), GATA binding protein 4 (GATA4) and SOX17 (endoderm) were expressed in the differentiated cells (Supplementary Fig. S3A) and there were no significant differences found between the three iPSCs. In addition, teratomas, which contained neural epithelium and melanocyte epithelium (ectoderm), cartilage (mesoderm), and gut epithelium (endoderm), were detected 2 months after iPSCs were injected into NOD-SCID mice (Fig. 2B). Immunostaining revealed that all the teratomas consisted of human cells, which clearly show that the tumors were of iPSC origin (Supplementary Fig. S3B). Both EB differentiation and teratoma formation demonstrated that all three of the reprogrammed iPS clones had the developmental potential to give rise to differentiated derivatives of all three primary germ layers.

Quantitative RT−PCR for the four transgenes revealed that OCT4, SOX2, NANOG and LIN28 were integrated into all three of the iPS clones and the relative integrated copies were 5−13. The integrated copies and the proportion of the four transgenes varied for each of the iPS clones (Supplementary Fig. S4). RT−PCR results showed that the expression of the endogenous OCT4, SOX2, NANOG and LIN28 was at levels similar to that of human ES cells, and the exogenous expression of these genes was silenced significantly after 20 passages (Fig. 2D). As described in a previous study (Papapetrou et al., 2009), pronounced lentivector silencing is a characteristic of successfully reprogrammed iPSC clones. Thus, our results suggest the successful reprogramming of POI1-iPSCs, POI2-iPSCs and hEF-iPSCs. More importantly, each of the three iPS clones had the same karyotypes as their cognate fibroblast cells, suggesting the chromosomal stability throughout the reprogramming process (Supplementary Fig. S5).

VASA-GFP-transduced iPSCs and induction of germ cell differentiation

Based on previous studies indicating that VASA is specifically expressed in germ cell lineage in both mice (Fujiwara et al., 1994) and humans (Castrillon et al., 2000), we introduced a GFP-conjugated VASA reporter into undifferentiated iPSCs. The transduced iPSCs were selected in CM with geneticin for 15 days. After selection, we prepared sublines. The subclone formation efficiency of POI1-iPSCs, POI2-iPSCs and hEF-iPSCs
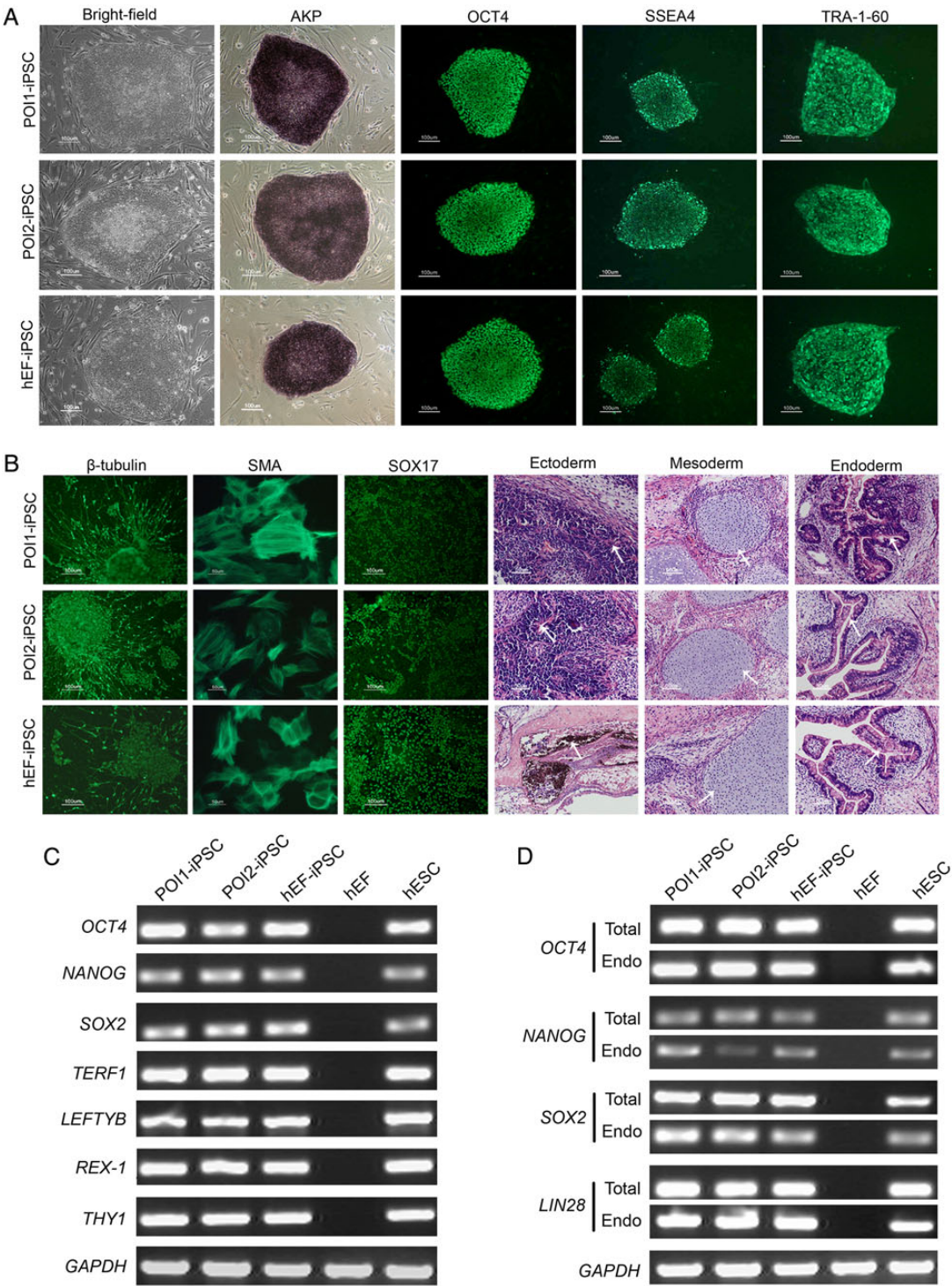
Figure 2 Characterization of induced pluripotent stem cell (iPSC) clones from primary ovarian insufficiency (POI) patients and healthy donor. (**A**) POI1-iPSCs, POI2-iPSCs, and normal human embryonic fibroblast (hEF)-iPSCs morphology, Alkaline phosphatase (AKP) staining, and immunofluorescence staining using anti-OCT4, -SSEA4, and -TRA-1−60 antibodies. Scale bars, 100 μm. (**B**) Immunostaining of differentiated cells from embryoid bodies (EBs) formed by POI1-iPSCs, POI2-iPSCs, and hEF-iPSCs using antibodies against β-tubulin (ectoderm), SMA (mesoderm), and SOX17 (endoderm). Scale bars, 100 μm. Hematoxylin and eosin staining of teratoma sections from POI1-iPSCs, POI2-iPSCs and hEF-iPSCs. Neural epithelium and melanocyte epithelium (ectoderm), cartilage (mesoderm), and gut epithelium (endoderm) are shown, as indicated by arrow. Scale bars, 50 μm. (**C**) RT−PCR assays for the expression of pluripotency-associated markers in POI1-iPSCs, POI2-iPSCs and hEF-iPSCs. (**D**) Endogenous (Endo) and total (Total) expression levels of OCT4, NANOG, SOX2 and LIN28 were analyzed with semiquantitative RT−PCR and compared with that in hEFs and human embryonic stem cells (hESCs). GAPDH was used as the positive control.

was 8.34, 12.5 and 8.34%, respectively (data not shown). Three sublines (POI1-iPS-V.1, POI2-iPS-V.1 and hEF-iPS-V.1) that stably transfected with the VASA-GFP reporter were selected from each of iPSCs. Immunostaining and quantitative RT–PCR revealed that each of the three subline maintained pluripotency after transduced with the VASA-GFP reporter (Supplementary Fig. S6A). aCGH assays showed that the POI1-iPS-V.1 and POI2-iPS-V.1 karyotype was consistent with that of the POI patients: arr (1–22) × 2, Xq26.3q28 (133, 934, 220–154, 500, 683) × 1 and arr (1–22) × 2, Xq26.3q28 (133, 934, 220–154, 500, 683) × 1, whereas hEF-iPS-V.1 had the normal karyotype of arr
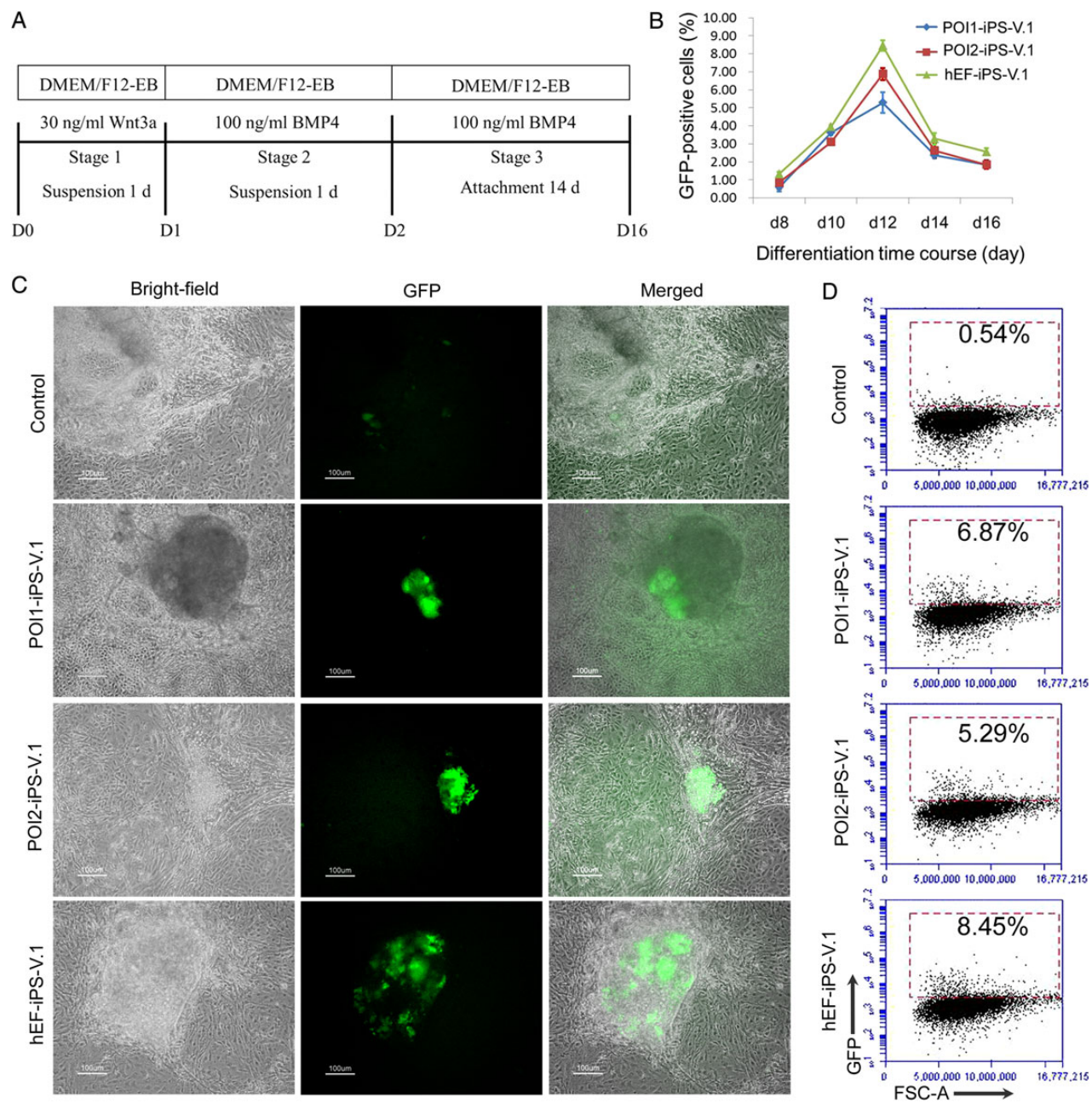

Figure 3 Potential of induced pluripotent stem cells (iPSC) derived from women with primary ovarian insufficiency (POI) (POI1-iPS-V.1, POI2-iPS-V.1), and from normal human embryonic fibroblasts (hEFs) (hEF-iPS-V.1), to differentiate into germ cell lineages. (**A**) Flow diagram of germ cell differentiation. (**B**) Fluorescence-activated cell sorting (FACS) analysis of the percentage of green fluorescent protein (GFP)-positive population at the various time points of differentiation. Error bars indicate SD, $n = 3$ (averages from three independently differentiated samples). (**C**) Adherent monolayer differentiation of POI1-iPS-V.1, POI2-iPS-V.1 and hEF-iPS-V.1 stably transfected with VASA-GFP construct. Bright field images depict structures arising during the 12-day differentiation with associated appearance of GFP-positive fluorescent cells by epifluorescence microscopy. Control cells were differentiated from hEF-iPS-V.1 without the addition of Wnt3a and bone morphogenetic protein 4 (BMP4). Scale bars, 100 μm. (**D**) FACS analysis of GFP populations differentiated from POI1-iPS-V.1, POI2-iPS-V.1 and hEF-iPS-V.1 at 12 days.

(1–22, X) × 2 (Supplementary Fig. S6B). These data indicate that the POI1-iPS-V.1, POI2-iPS-V.1 and hEF-iPS-V.1 sublines maintained stable karyotypes from their original fibroblasts.

We next explored the possibility of differentiating POI1-iPS-V.1, POI2-iPS-V.1 and hEF-iPS-V.1 into germ cell lineages and used the VASA-GFP reporter to purify germ cells from the complex cell mixture. Previous studies had demonstrated that Wnt3a and BMPs promote differentiation of hESCs or iPSCs to germ cells *in vitro* (Kee et al., 2009; Panula et al., 2011; Wei et al., 2008). To this end, we treated POI1-iPS-V.1, POI2-iPS-V.1, and hEF-iPS-V.1 with BMP4 and Wnt3a to induce germ cell differentiation (Fig. 3A), finding that all three sublines produced green fluorescent cells in the differentiated cultures. The fluorescent cells appeared after a minimum culture time of 8 days, and the number of green fluorescent areas in the cultures increased substantially and reached an apparent peak at Day 12, disappearing at Day 16 (Fig. 3B). In the differentiated cultures (Days 10–14), green

fluorescent cells were observed in larger, organized aggregates that were frequently raised above the monolayer (Fig. 3C). After digesting the differentiated monolayer into single cells, GFP-positive and GFP-negative cells were enriched by FACS. The percentage of GFP-positive cells increased over 12 days of differentiation by a maximum 6.87 ± 0.33%, 5.29 ± 0.57% and 8.45 ± 0.29% in POI1-iPS-V.1, POI2-iPS-V.1 and hEF-iPS-V.1, respectively (Fig. 3D), whereas the baseline percentages of GFP-positive cells in undifferentiated cultures were similar and very low (0.54%, 0.37%, 0.62%, respectively) (data not shown). Following sorting, we analyzed GFP-positive and GFP-negative cells for VASA (immunostaining) and for germ cell markers (quantitative RT–PCR). Immunostaining confirmed that GFP-positive cells were enriched for endogenous VASA protein, whereas GFP-negative cells had very low or no endogenous VASA expression. VASA protein was localized specifically to the cytoplasm of the GFP-positive cells (Fig. 4A). Further analysis showed that early germ
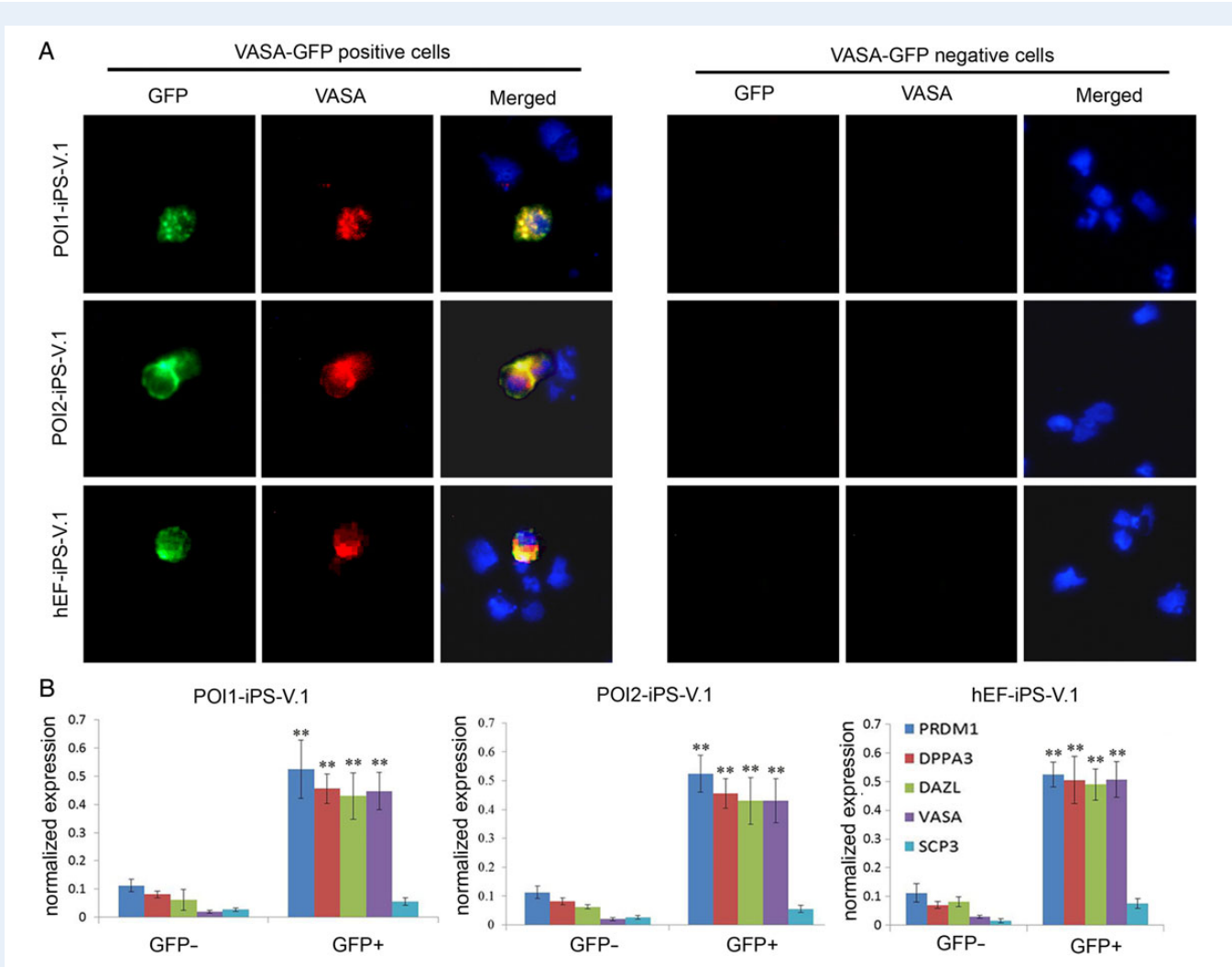
Figure 4 Detailed characterization of sorted Asp-Glu-Ala-Asp box polypeptide 4-green fluorescent protein (VASA-GFP) positive and negative cells. (**A**) Immunostaining of VASA in sorted VASA-GFP positive and VASA-GFP negative cells (Day 12 of differentiation with Wnt3a and bone morphogenic protein 4 (BMP4)) shows cytoplasm VASA staining in some VASA-GFP positive cells, but VASA-GFP negative cells do not show VASA staining. (**B**) Quantitative RT–PCR determination of early germ cell markers expression in sorted VASA-GFP positive and VASA-GFP negative cells (Day 12 of differentiation with Wnt3a and BMP4). Error bars indicate SD; asterisk, significant difference by t-test ($P < 0.01$), $n = 3$ (averages from three independently differentiated samples at 12 days).

cell markers such as PR domain containing 1 with ZNF domain (*PRDM1*, *BLIMP1*), developmental pluripotency-associated 3 (*DPPA3*, *STELLA*), deleted in azoospermia-like (*DAZL*), and *VASA* (*DDX4*) were significantly enriched in the GFP-positive population, whereas the expression of synaptonemal complex protein 3 (*SCP3*), typically expressed during the later stages of germ cell development, was almost undetected in the GFP-positive population (Fig. 4B). These results indicate that the GFP-positive cells were probably pre-meiotic PGCs. Thus, our results suggest that early-stage germ cells can be differentiated and isolated from POI1-iPS-V.1, POI2-iPS-V.1 and hEF-iPS-V.1.

A

Gene Symbol	Gene Title	Location	Fold change ([positive] vs [negative])
RAB39B	RAB39B, member RAS oncogene family	Xq28	25.532915
IKBKG	inhibitor of kappa light polypeptide gene enhancer in B-cells, kinase gamma	Xq28	19.556517
RP1-177G6.2	hypothetical protein LOC286411	Xq27.1	13.254381
FAM122C	family with sequence similarity 122C	Xq26.3	7.199228
RBMX	RNA binding motif protein, X-linked	Xq26.3	5.938829
MAMLD1	mastermind-like domain containing 1	Xq28	4.2316847
PASD1	PAS domain containing 1	Xq28	3.750382
F8	coagulation factor VIII, procoagulant component	Xq28	3.4912286
MAGEA3	melanoma antigen family A, 3	Xq28	3.0440576
VGLL1	Vestigial-like family member 1	Xq26.3	3.015912
SLITRK4	SLIT and NTRK-like family, member 4	Xq27.3	2.5850725
IDS	iduronate 2-sulfatase	Xq28	2.4159253
CLIC2	chloride intracellular channel 2	Xq28	2.3689725
FGF13	fibroblast growth factor 13	Xq26.3	2.3048198
ATP11C	ATPase, class VI, type 11C	Xq27.1	2.298014
TMLHE	trimethyllysine hydroxylase, epsilon	Xq28	2.260178
ARHGEF6	Rac/Cdc42 guanine nucleotide exchange factor (GEF) 6	Xq26.3	2.1862214
BRCC3	BRCA1/BRCA2-containing complex, subunit 3	Xq28	2.1793904
PNMA6A	Paraneoplastic Ma antigen family member 6A	Xq28	2.1086228

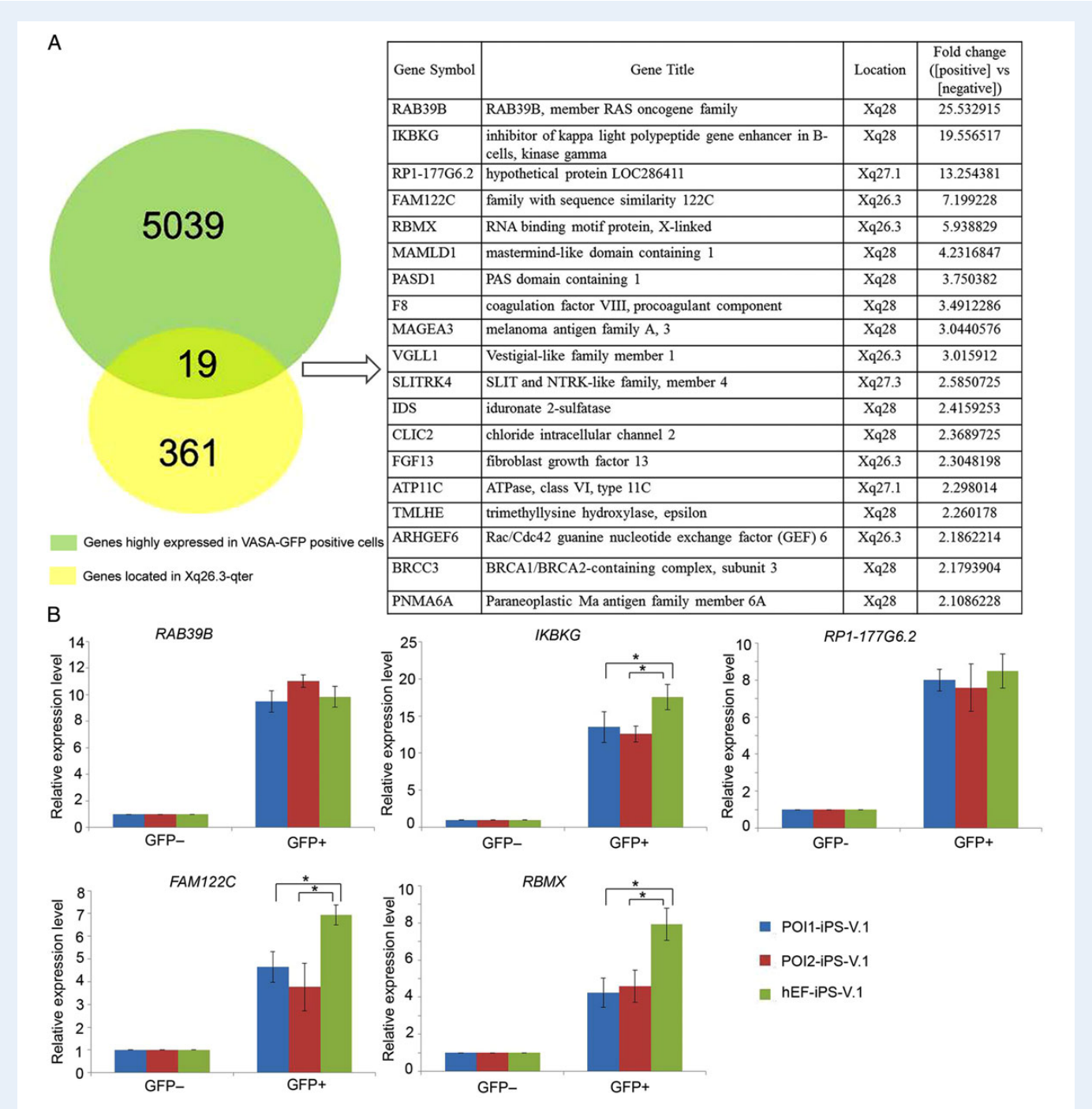**Figure 5** Gene expression analyzed within Xq26.3-q28. (**A**) Venn diagrams showing the numbers of genes highly expressed in Asp-Glu-Ala-Asp box polypeptide 4-green fluorescent protein (VASA-GFP) positive cells and genes located in the deleted region of Xq26.3-q28. (**B**) Quantitative RT−PCR analysis of expression levels of the five potential candidate genes in VASA-GFP positive and VASA-GFP negative cells (Day 12 of differentiation with Wnt3a and bone morphogenetic protein 4 (BMP4)). The value of each gene in GFP-population was set to 1. Error bars indicate SD; asterisk, significant difference by t-test ($P < 0.05$), $n = 3$ (averages from three independently differentiated samples at 12 days).

Gene expression in Xq26.3–q28

Chromosomal analysis in our study have identified that there was an Xq26.3–q28 deletion in the POI patients. A total of 361 genes are identified within this region through searching in the Database of Human Genome. On the basis of a previous study, 5, 039 genes were found to have more than 2-fold increase in the expression of VASA-GFP positive cells when compared with VASA-GFP negative (Tilgner et al., 2010). Nineteen genes are located on the deleted X chromosome region, from which five potential candidate genes with more than 5-folds change were selected for analysis in our POI-iPS model. The five genes included RAB39B, inhibitor of kappa light polypeptide gene enhancer in B-cells, kinase gamma (IKBKG), hypothetical protein LOC286411 (RP1-177G6.2), family with sequence similarity 122C (FAM122C), and RNA binding motif protein, X-linked (RBMX) (Fig. 5A). We observed that GFP-positive cells were enriched for expression of RAB39B, IKBKG, RP1-177G6.2, FAM122C and RBMX ($P < 0.05$), which was consistent with previous report of their expression in VASA-GFP positive cells (Tilgner et al., 2010). Moreover, the GFP-positive cells differentiated from POI-iPSCs had reduced expression of FAM122C, RBMX and IKBKG than cells from normal iPSCs ($P < 0.05$) (Fig. 5B). Therefore, our results indicate that X chromosome deletion would cause altered expression of genes related to germ cell differentiation located in the deleted region.

Discussion

We generated two iPSC lines from POI patients with X chromosome microdeletion. The iPSCs were similar to hESCs in many aspects, including morphology, expression of pluripotency-associated genes, in vitro differentiation, and teratoma formation. Furthermore, we verified that the POI-iPSCs could differentiate into germ cells following the addition of BMP4 and Wnt3a. To the best of our knowledge, this is the first study of the germ cell differentiation potential of iPSCs from POI. The findings obtained here pave the way for future elucidation of the molecular mechanisms of POI and the development of novel therapies for POI.

Lentiviral 4-factor (OCT4, SOX2, NANOG, LIN28) system was previously demonstrated to successful reprogram somatic cells (Yu et al., 2007). Using this system, we generated iPSCs from POI and healthy fibroblasts in the efficiency less than 0.01%. We found that each iPS clone we analyzed contained 5 to 13 copies of each factor, and the proportion of integrated copies of the four factors also varied in each of the iPS clones. But interestingly, we did not observe significant differences in both the pluripotency and self-renewal ability among these iPSC lines. We suggested that the three iPSC lines we analyzed were selected through long-term culture and undergo completely reprograming, at this stage the integrated factors may silenced and had little influence on the iPS characters. This was in accordance with the RT–PCR results, which confirmed strong silencing of all the four transgenic genes in the stably expanded reprogrammed cells, indicating that these iPS cells are efficiently reprogrammed and do not depend on continuous expression of the four transgenes for self-renewal. Stable VASA-GFP reporter transfection into hESCs or iPSCs has been reported based on the specificity of VASA as a germ cell marker in vivo (Kee et al., 2009). Some studies have shown that the VASA-GFP reporter traces differentiated germ cells effectively in vitro. In our study, POI1-iPS-V.1, POI2-iPS-V.1 and hEF-iPS-V.1 all produced green fluorescent cells after 12 days of

differentiation, and the percentage of GFP-positive cells was similar between POI1-iPS-V.1 and POI2-iPS-V.1 and were slightly lower than hEF-iPS-V.1. One possibility was that the partial Xq deletion reduced the germ cell differentiation potential. However, several investigators have suggested that cellular changes resulting from reprogramming process or genetic background variability can result in individual iPSC lines displaying variable biological properties (Bock et al., 2011; Boulting et al., 2011; Kim and Svendsen, 2011). Thus, more iPSC lines should be assessed before a truly representative and faithfully reprogrammed iPSC-based disease model is established. Our results are based on two iPSC lines derived from two different POI patients. Therefore, the less efficient potential for differentiating into germ cells of the two lines might indicate chromosomal abnormalities as the possible etiology.

Previous cytogenetic and molecular characterization of X chromosomes in women with POI has defined two critical regions for POI: POI1 Xq26-q28 and POI2 Xq13.3-q22 (Sala et al., 1997; Portnoi et al., 2006; De Vos et al., 2010; Jiao et al., 2012). Numerous studies have identified a group of candidate genes for POI, including FMR1 (309550) (Coulam et al., 1986), FMR2 (300806) (Persani et al., 2010), POF1B (300603) (Dixit et al., 2010) and DACH2 (300608) (Berletch et al., 2011). However, the function of these genes in ovarian physiology remains unclear, and these genes were insufficient to explain the correlations between the incidence of POI and X chromosomal deletion. Ferreira et al. (Ferreira et al., 2010) suggested that the molecular mechanism leading to the POI phenotype could be due to haploinsufficiency of ovarian-related genes located within the deleted regions and usually escaping X inactivation. Here, we found that the expression level of several genes located in the deletion region of the X chromosome and previously proven to be highly expressed in differentiated germ cells (Tilgner et al., 2010) were significantly lower in POI-iPSC-derived PGCs. Thus, we speculated that these genes might be possible candidate genes for POI. RBMX is an active X chromosome homolog of the Y chromosome RBMY gene and is located in the critical area of POI (Xq26.3) (Delbridge et al., 1999). RBMY evolves a male-specific function in spermatogenesis (Abid et al., 2013); RBMY deletion corresponds to azoospermia or severe oligozoospermia. RBMX expression is biallelic and escapes X chromosome inactivation (Delbridge et al., 1999), which indicates that Xq26.3-q28 deletion might result in reduced RBMX expression. Recently, it was reported that RBMX plays a role in cell division and may be related to apoptosis (Adamson et al., 2012; Matsunaga et al., 2012). In this study, POI-iPSCs exhibited reduced germ cell differentiation potential and lower expression of FAM122C, RBMX and IKBKG compared with that of normal iPSCs, whether this phenotype was at least partially due to the three genes requires further investigation.

In conclusion, our results indicate that human germ cells can be differentiated and isolated from POI-iPSCs. Moreover, we observed that GFP-positive cells differentiated from POI-iPSCs had reduced expression of FAM122C, RBMX and IKBKG, located in the deleted region of the X chromosome and highly expressed in differentiated germ cells, compared with normal iPSCs. The availability of POI-iPSCs and their utilization in disease modeling will accelerate our understanding, diagnosis, and treatment of POI.

Supplementary data

Supplementary data are available at http://humrep.oxfordjournals.org/.

Acknowledgements

Authors' roles

G.L. and G.-X.L. conceived the study, provided financial support and revised the manuscript. L.-Z.L. performed the germ cell differentiation and related testing, analyzed the data and wrote the paper. Y.-Q.T. performed the aCGH assays and karyotype analysis and interpreted the results. F.G. recruited patients and signed the consent form. L.H., Y.Z. and Q.O.-Y. carried out the experiments for the generation of iPSC and tested the pluripotency of the iPSC.

Funding

Conflict of interest

None declared.

References

Abid S, Sagare-Patil V, Gokral J, Modi D. Cellular ontogeny of RBMY during human spermatogenesis and its role in sperm motility. *J Biosci* 2013; **38**:85–92.

Adamson B, Smogorzewska A, Sigoillot FD, King RW, Elledge SJ. A genome-wide homologous recombination screen identifies the RNA-binding protein RBMX as a component of the DNA-damage response. *Nat Cell Biol* 2012;**14**:318–328.

Bachner D, Manca A, Steinbach P, Wohrle D, Just W, Vogel W, Hameister H, Poustka A. Enhanced expression of the murine FMR1 gene during germ cell proliferation suggests a special function in both the male and the female gonad. *Hum Mol Genet* 1993;**2**:2043–2050.

Baronchelli S, Conconi D, Panzeri E, Bentivegna A, Redaelli S, Lissoni S, Saccheri F, Villa N, Crosti F, Sala E *et al.* Cytogenetics of premature ovarian failure: an investigation on 269 affected women. *J Biomed Biotechnol* 2011;**2011**:370195.

Berletch JB, Yang F, Xu J, Carrel L, Disteche CM. Genes that escape from X inactivation. *Hum Genet* 2011;**130**:237–245.

Bione S, Sala C, Manzini C, Arrigo G, Zuffardi O, Banfi S, Borsani G, Jonveaux P, Philippe C, Zuccotti M *et al.* A human homologue of the Drosophila melanogaster diaphanous gene is disrupted in a patient with premature ovarian failure: evidence for conserved function in oogenesis and implications for human sterility. *Am J Hum Genet* 1998;**62**:533–541.

Bione S, Rizzolio F, Sala C, Ricotti R, Goegan M, Manzini MC, Battaglia R, Marozzi A, Vegetti W, Dalpra L *et al.* Mutation analysis of two candidate genes for premature ovarian failure, DACH2 and POF1B. *Hum Reprod* 2004;**19**:2759–2766.

Bock C, Kiskinis E, Verstappen G, Gu H, Boulting G, Smith ZD, Ziller M, Croft GF, Amoroso MW, Oakley DH *et al.* Reference Maps of human ES and iPS cell variation enable high-throughput characterization of pluripotent cell lines. *Cell* 2011;**144**:439–452.

Boulting GL, Kiskinis E, Croft GF, Amoroso MW, Oakley DH, Wainger BJ, Williams DJ, Kahler DJ, Yamaki M, Davidow L *et al.* A functionally characterized test set of human induced pluripotent stem cells. *Nat Biotechnol* 2011;**29**:279–286.

Castillo S, Lopez F, Tobella L, Salazar S, Daher V. The cytogenetics of premature ovarian failure. *Rev Chil Obstet Ginecol* 1992;**57**:341–345.

Castrillon DH, Quade BJ, Wang TY, Quigley C, Crum CP. The human VASA gene is specifically expressed in the germ cell lineage. *Proc Natl Acad Sci USA* 2000;**97**:9585–9590.

Ceylaner G, Altinkaya SO, Mollamahmutoglu L, Ceylaner S. Genetic abnormalities in Turkish women with premature ovarian failure. *Int J Gynaecol Obstet* 2010;**110**:122–124.

Chamberlain SJ, Chen PF, Ng KY, Bourgois-Rocha F, Lemtiri-Chlieh F, Levine ES, Lalande M. Induced pluripotent stem cell models of the genomic imprinting disorders Angelman and Prader-Willi syndromes. *Proc Natl Acad Sci USA* 2010;**107**:17668–17673.

Christin-Maitre S, Braham R. General mechanisms of premature ovarian failure and clinical check-up. *Gynecol Obstet Fertil* 2008; **36**:857–861.

Cordts EB, Christofolini DM, Dos Santos AA, Bianco B, Barbosa CP. Genetic aspects of premature ovarian failure: a literature review. *Arch Gynecol Obstet* 2011;**283**:635–643.

Coulam CB. Premature gonadal failure. *Fertil Steril* 1982;**38**:645–655.

Coulam CB, Adamson SC, Annegers JF. Incidence of premature ovarian failure. *Obstet Gynecol* 1986;**67**:604–606.

Davison RM, Fox M, Conway GS. Mapping of the POF1 locus and identification of putative genes for premature ovarian failure. *Mol Hum Reprod* 2000;**6**:314–318.

De Vos M, Devroey P, Fauser BC. Primary ovarian insufficiency. *Lancet* 2010; **376**:911–921.

Delbridge ML, Lingenfelter PA, Disteche CM, Graves JA. The candidate spermatogenesis gene RBMY has a homologue on the human X chromosome. *Nat Genet* 1999;**22**:223–224.

Dimos JT, Rodolfa KT, Niakan KK, Weisenthal LM, Mitsumoto H, Chung W, Croft GF, Saphier G, Leibel R, Goland R *et al.* Induced pluripotent stem cells generated from patients with ALS can be differentiated into motor neurons. *Science* 2008;**321**:1218–1221.

Dixit H, Rao L, Padmalatha V, Raseswari T, Kapu AK, Panda B, Murthy K, Tosh D, Nallari P, Deenadayal M *et al.* Genes governing premature ovarian failure. *Reprod Biomed Online* 2010;**20**:724–740.

Ebert AD, Yu J, Rose FF Jr., Mattis VB, Lorson CL, Thomson JA, Svendsen CN. Induced pluripotent stem cells from a spinal muscular atrophy patient. *Nature* 2009;**457**:277–280.

Ferreira SI, Matoso E, Pinto M, Almeida J, Liehr T, Melo JB, Carreira IM. X-chromosome terminal deletion in a female with premature ovarian failure: haploinsufficiency of X-linked genes as a possible explanation. *Mol Cytogenet* 2010;**3**:14.

Forges T, Monnier-Barbarino P, Leheup B, Jouvet P. Pathophysiology of impaired ovarian function in galactosaemia. *Hum Reprod Update* 2006; **12**:573–584.

Fujiwara Y, Komiya T, Kawabata H, Sato M, Fujimoto H, Furusawa M, Noce T. Isolation of a DEAD-family protein gene that encodes a murine homolog of Drosophila vasa and its specific expression in germ cell lineage. *Proc Natl Acad Sci USA* 1994;**91**:12258–12262.

Gleicher N, Weghofer A, Barad DH. A pilot study of premature ovarian senescence: I. Correlation of triple CGG repeats on the FMR1 gene to ovarian reserve parameters FSH and anti-Mullerian hormone. *Fertil Steril* 2009;**91**:1700–1706.

Janse F, Knauff EA, Niermeijer MF, Eijkemans MJ, Laven JS, Lambalk CB, Fauser BC, Goverde AJ; Dutch Premature Ovarian Failure Consortium. Similar phenotype characteristics comparing familial and sporadic premature ovarian failure. *Menopause* 2010;**17**:758–765.

Jiao X, Qin C, Li J, Qin Y, Gao X, Zhang B, Zhen X, Feng Y, Simpson JL, Chen ZJ. Cytogenetic analysis of 531 Chinese women with premature ovarian failure. *Hum Reprod* 2012;**27**:2201–2207.

Kee K, Angeles VT, Flores M, Nguyen HN, Reijo Pera RA. Human DAZL, DAZ and BOULE genes modulate primordial germ-cell and haploid gamete formation. *Nature* 2009;**462**:222–225.

Kim HW, Svendsen CN. Gene editing in stem cells hits the target. *Cell Stem Cell* 2011;**9**:93–94.

Lin G, Xie Y, Ouyang Q, Qian X, Xie P, Zhou X, Xiong B, Tan Y, Li W, Deng L et al. HLA-matching potential of an established human embryonic stem cell bank in China. *Cell Stem Cell* 2009;**5**:461–465.

Lorda-Sanchez IJ, Ibanez AJ, Sanz RJ, Trujillo MJ, Anabitarte ME, Querejeta ME, Rodriguez de Alba M, Gimenez A, Infantes F, Ramos C et al. Choroideremia, sensorineural deafness, and primary ovarian failure in a woman with a balanced X-4 translocation. *Ophthalmic Genet* 2000;**21**:185–189.

Mansouri MR, Schuster J, Badhai J, Stattin EL, Losel R, Wehling M, Carlsson B, Hovatta O, Karlstrom PO, Golovleva I et al. Alterations in the expression, structure and function of progesterone receptor membrane component-1 (PGRMC1) in premature ovarian failure. *Hum Mol Genet* 2008; **17**:3776–3783.

Marchetto MC, Carromeu C, Acab A, Yu D, Yeo GW, Mu Y, Chen G, Gage FH, Muotri AR. A model for neural development and treatment of Rett syndrome using human induced pluripotent stem cells. *Cell* 2010; **143**:527–539.

Matsunaga S, Takata H, Morimoto A, Hayashihara K, Higashi T, Akatsuchi K, Mizusawa E, Yamakawa M, Ashida M, Matsunaga TM et al. RBMX: a regulator for maintenance and centromeric protection of sister chromatid cohesion. *Cell Rep* 2012;**1**:299–308.

Nippita TA, Baber RJ. Premature ovarian failure: a review. *Climacteric* 2007; **10**:11–22.

Nishimura-Tadaki A, Wada T, Bano G, Gough K, Warner J, Kosho T, Ando N, Hamanoue H, Sakakibara H, Nishimura G et al. Breakpoint determination of X;autosome balanced translocations in four patients with premature ovarian failure. *J Hum Genet* 2011;**56**:156–160.

Panula S, Medrano JV, Kee K, Bergstrom R, Nguyen HN, Byers B, Wilson KD, Wu JC, Simon C, Hovatta O et al. Human germ cell differentiation from fetal- and adult-derived induced pluripotent stem cells. *Hum Mol Genet* 2011;**20**:752–762.

Papapetrou EP, Tomishima MJ, Chambers SM, Mica Y, Reed E, Menon J, Tabar V, Mo Q, Studer L, Sadelain M. Stoichiometric and temporal requirements of Oct4, Sox2, Klf4, and c-Myc expression for efficient human iPSC induction and differentiation. *Proc Natl Acad Sci USA* 2009;**106**:12759–12764.

Pasca SP, Portmann T, Voineagu I, Yazawa M, Shcheglovitov A, Pasca AM, Cord B, Palmer TD, Chikahisa S, Nishino S et al. Using iPSC-derived neurons to uncover cellular phenotypes associated with Timothy syndrome. *Nat Med* 2011;**17**:1657–1662.

Persani L, Rossetti R, Cacciatore C. Genes involved in human premature ovarian failure. *J Mol Endocrinol* 2010;**45**:257–279.

Portnoi MF, Aboura A, Tachdjian G, Bouchard P, Dewailly D, Bourcigaux N, Frydman R, Reyss AC, Brisset S, Christin-Maitre S. Molecular cytogenetic studies of Xq critical regions in premature ovarian failure patients. *Hum Reprod* 2006;**21**:2329–2334.

Prueitt RL, Chen H, Barnes RI, Zinn AR. Most X;autosome translocations associated with premature ovarian failure do not interrupt X-linked genes. *Cytogenet Genome Res* 2002;**97**:32–38.

Rao Kandukuri L, Padmalatha V, Kanakavalli M, Turlapati R, Swapna M, Vidyadhari M, Saranaya G, Himaja K, Deenadayal M, Kumar Sethi B et al. Unique case reports associated with ovarian failure: necessity of two intact x chromosomes. *Case Rep Genet* 2012;**2012**:640563.

Rife M, Nadal A, Mila M, Willemsen R. Immunohistochemical FMRP studies in a full mutated female fetus. *Am J Med Genet A* 2004;**124A**:129–132.

Rizzolio F, Pramparo T, Sala C, Zuffardi O, De Santis L, Rabellotti E, Calzi F, Fusi F, Bellazzi R, Toniolo D. Epigenetic analysis of the critical region I for premature ovarian failure: demonstration of a highly heterochromatic domain on the long arm of the mammalian X chromosome. *J Med Genet* 2009;**46**:585–592.

Sala C, Arrigo G, Torri G, Martinazzi F, Riva P, Larizza L, Philippe C, Jonveaux P, Sloan F, Labella T et al. Eleven X chromosome breakpoints associated with premature ovarian failure (POF) map to a 15-Mb YAC contig spanning Xq21. *Genomics* 1997;**40**:123–131.

Sinha P, Kuruba N. Premature ovarian failure. *J Obstet Gynaecol* 2007; **27**:16–19.

Tharapel AT, Anderson KP, Simpson JL, Martens PR, Wilroy RS Jr., Llerena JC Jr., Schwartz CE. Deletion (X)(q26.1-->q28) in a proband and her mother: molecular characterization and phenotypic-karyotypic deductions. *Am J Hum Genet* 1993;**52**:463–471.

Tilgner K, Atkinson SP, Yung S, Golebiewska A, Stojkovic M, Moreno R, Lako M, Armstrong L. Expression of GFP under the control of the RNA helicase VASA permits fluorescence-activated cell sorting isolation of human primordial germ cells. *Stem Cells* 2010;**28**:84–92.

Wei W, Qing T, Ye X, Liu H, Zhang D, Yang W, Deng H. Primordial germ cell specification from embryonic stem cells. *PLoS One* 2008;**3**:e4013.

Yu J, Vodyanik MA, Smuga-Otto K, Antosiewicz-Bourget J, Frane JL, Tian S, Nie J, Jonsdottir GA, Ruotti V, Stewart R et al. Induced pluripotent stem cell lines derived from human somatic cells. *Science* 2007;**318**:1917–1920.

Zhou J, Ou-Yang Q, Li J, Zhou XY, Lin G, Lu GX. Human feeder cells support establishment and definitive endoderm differentiation of human embryonic stem cells. *Stem Cells Dev* 2008;**17**:737–749.